Research in Astronomy and Astrophysics, 23:055005 (8pp), 2023 May https://doi.org/10.1088/1674-4527/acc506

The First Multiband Photometric Light Curve Solutions of the V Gru Binary System from the Southern Hemisphere

Mehmet Tanriver[1,2], Atila Poro[3], Ahmet Bulut[4,5], Ahmet Keskin[1], and Mark G. Blackford[6]
[1] Department of Astronomy and Space Science, Faculty of Science, University of Erciyes, TR-38039, Kayseri, Türkiye
[2] Erciyes University, Astronomy and Space Science Observatory Application and Research Center, TR-38039, Kayseri, Türkiye
[3] Astronomy Department of the Raderon AI Lab., BC., Burnaby, Canada; poroatila@gmail.com
[4] Department of Physics, Faculty of Science, Çanakkale Onsekiz Mart University, Terzioğlu Kampüsü, TR-17020, Çanakkale, Türkiye
[5] Astrophysics Research Center and Ulupınar Observatory, Çanakkale Onsekiz Mart University, TR-17020, Çanakkale, Türkiye
[6] Variable Stars South (VSS), Congarinni Observatory, Congarinni, NSW, 2447, Australia
Received 2022 November 9; revised 2023 March 6; accepted 2023 March 15; published 2023 April 17

Abstract

The first multiband photometric solutions of the short-period V Gru eclipsing binary from the southern hemisphere are presented in this study. Light curves of the system were observed through *BVI* filters at the Congarinni Observatory in Australia for 15 nights. In addition to the new ground-based data, we also used the TESS observations in two sectors. We analyzed the light curves of the system using the PHysics Of Eclipsing BinariEs (PHOEBE) 2.4.7 version code to achieve the best accordance with the photometric observations. The solutions suggest that V Gru is a near-contact binary system with $q = 1.302(81)$ mass ratio, $f_1 = 0.010(23)$, $f_2 = -0.0.009$ (21), and $i = 73.45(38)$. We considered the two hot spots on the hotter and cooler components for the light curve analysis. We extracted the minima times from the light curves based on the Markov Chain Monte Carlo (MCMC) approach. Using our new light curves, TESS, and additional literature minima, we computed the ephemeris of V Gru. The system's eclipse timing variation trend was determined using the MCMC method. This system is a good and challenging case for future studies.

Key words: (stars:) binaries: eclipsing – techniques: photometric – stars: individual (V Gru)

1. Introduction

Regarding the type of V Gru system in the binary stars' categories, contradictory cases are mentioned in the catalogs. In the Washington double star (WDS) catalog and the AAVSO international variable star index (VSX), V Gru was classified as a W UMa contact system type (Mason et al. 2001). This binary system is classified as a β Lyrae in the machine-learned All Sky Automated Survey (ASAS) classification catalog (Richards et al. 2012). The review history of this system fully shows its complexity.

Leavitt & Pickering (1913) identified V Gru as a new southern variable star with the name HV 3365. They stated that HV 3365 is an Algol or β Lyr type binary system with an apparent magnitude of $V = 9.55$. V Gru is indicated by Houk (1978) in the Michigan Catalog of HD stars Vol-2 as HD 207697. Wolf et al. (1982) presented the first minimum time of V Gru. Wolf & Kern (1983) published the V, $b-y$, m_1, c_1, and H_β values of the V Gru binary system in a photometric survey of the southern hemisphere eclipsing binary stars on nine different Julian days, and they also determined the period of the system as 0.4833 days. Giuricin et al. (1983) classified this system as a contact or a typical semi-detached configuration, evolved, fairly close binary system. Budding (1984) gave the possible mass ratios in the study, but he stated that the solution is ambiguous. Cannon & Pickering (1993) gave the photovisual and photographic magnitudes of V Gru as 9.80 and 9.50 respectively in the Henry Draper Catalogue and Extension. Demartino et al. (1996) reported the new coordinates of V Gru at that time in their study "Accurate Positions of Variable Stars Near the South Galactic Pole." Hauck & Mermilliod (1998) included V Gru in the *uvbyβ* photoelectric photometric catalog. Lopez & Lepez (2000) stated variables in the HIP, TYC, PPM, and AC catalogs. Budding et al. (2004) included V Gru in their catalog of Algol-type binary stars. Avvakumova et al. (2013) stated the orbital period of the V Gru binary system as 0.4834454954 days in the Catalogue of Eclipsing Variables (Version 2) and also gave the spectral type and the light curve type as F2V and EW respectively. Kordopatis et al. (2013) published heliocentric radial velocity as -19.0 ± 11.4 km s^{-1} in the RAdial Velocity Experiment (RAVE) Data Release 4 (DR4). Paunzen (2015) gave V magnitude and color indexes of V Gru in the Stroemgren-Crawford *uvbyβ* photometry catalog. Kunder et al. (2017) updated the heliocentric radial velocity as -18.973 ± 11.447 km s^{-1} in the RAVE Data Release 5 (DR5). The Cruzalèbes et al. (2019) study is included in the Mid-infrared stellar Diameters and Fluxes compilation Catalog (MDFC)-version 10. Steinmetz et al. (2020) updated the value of heliocentric radial velocity as -18.95 ± 11.34 km s^{-1} in RAVE Data Release 6 (DR6).

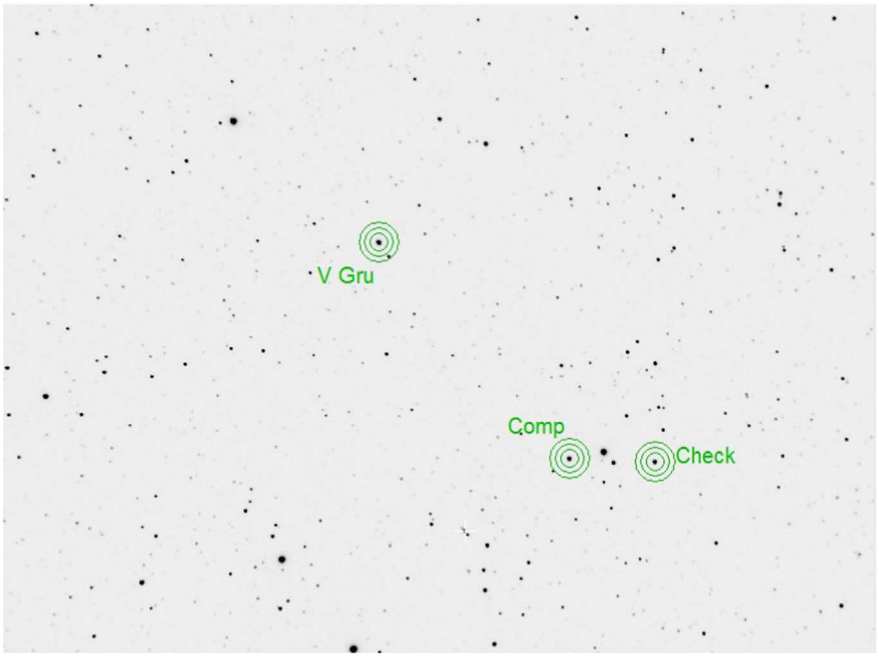

Figure 1. Observed field-of-view for V Gru, comparison star, and check star.

In this investigation, we analyze the light curves of the V Gru system. We obtained CCD observations with multi-bands at an observatory in Australia and optimally created binary star models suitable for these observations using the PHysics Of Eclipsing BinariEs (PHOEBE) code. The present study is the first in-depth and multiband photometric analysis of this system according to ground-based and space-based observations. Sections present observations, image reduction and instruments used, light curve analysis, the result of photometry, refind ephemeris, light curve behavior, spectral classification, and finally, conclusion.

2. Observation and Data Reduction

V Gru was observed for 15 nights in 2020 August with an Orion ED80T CF 80 mm refractor telescope at the Congarinni Observatory in Australia (152° 52′ East and 30° 44′ South). The data were taken using an Atik One 6.0 CCD camera with 1×1 binning and a CCD temperature of $-10°$ C. These observations were made using the Astrodon Johnson-Cousins *BVI* standard filters. TYC 7990-634-1 was selected as a comparison star and TYC 7989-722-1 was chosen as a check star with an appropriate apparent magnitude in comparison to V Gru. The comparison star was found at R.A. $21^{h}\ 50^{m}\ 20\overset{s}{.}93$, decl. 42° 41′ 46.″65 (J2000) with a $V = 10.291(22)$ magnitude, while the check star was located at R.A. $21^{h}\ 49^{m}\ 39\overset{s}{.}28$, decl. −42° 42′ 02.″91 (J2000) with a $V = 10.575(21)$ magnitude, according to the Simbad[7] astronomical database. Figure 1 shows the observed field-of-view for V Gru with the comparison and check stars. During the observations, a total of 1672 images were acquired. The CCD image processing was done with MaxIm DL software, which included dark, bias, and flat-field corrections (George 2000).

The Transiting Exoplanet Survey Satellite (TESS) mission observed the V Gru system in addition to our ground-based observations. TESS data are available at the Mikulski Archive for Space Telescopes (MAST).[8] The LightKurve code[9] was used to extract TESS style curves from MAST, which had been detrended using the TESS Science Processing Operations Center (SPOC) pipeline (Jenkins et al. 2016). TESS obtained these data in sectors 1 and 28, which were observed by camera 1 for a total of 55 days. We used the AstroImageJ (AIJ) program to normalize all of the ground-based and TESS data (Collins et al. 2017).

3. Light Curve Solutions

Photometric light curve analysis of the V Gru system was performed by Python Version 2.4.7 of PHOEBE (Prša & Zwitter 2005; Conroy et al. 2020; Poro et al. 2022). We first found a good fit based on all of the initial inputs and the appearance of the light curves. Aside from some initial inputs, the program searched for suitable values for mass ratio, orbital inclination, and star temperature ratio. Then the parameters

[7] http://simbad.u-strasbg.fr/simbad

[8] http://archive.stsci.edu/tess/all_products.html

[9] https://docs.lightkurve.org

Table 1
Light Curve Solutions of V Gru

Parameter	Result
$T_{\rm hotter}$ (K)	6749(89)
$T_{\rm cooler}$ (K)	5510(103)
$q = M_2/M_1$	1.302(81)
$\Omega_{\rm hotter}$	4.221(66)
$\Omega_{\rm cooler}$	4.268(47)
i°	73.45(38)
$f_{\rm hotter}$	0.010(23)
$f_{\rm cooler}$	−0.009(21)
$A_{\rm hotter} = A_{\rm cooler}$	0.50
$g_{\rm hotter} = g_{\rm cooler}$	0.32
$l_{\rm hotter}/l_{tot}$	0.667(2)
$l_{\rm cooler}/l_{tot}$	0.333(2)
$r_{\rm hotter}$(back)	0.430(2)
$r_{\rm hotter}$(side)	0.399(2)
$r_{\rm hotter}$(pole)	0.379(2)
$r_{\rm cooler}$(back)	0.374(3)
$r_{\rm cooler}$(side)	0.345(3)
$r_{\rm cooler}$(pole)	0.330(3)
$r_{\rm hotter}$(mean)	0.402(2)
$r_{\rm cooler}$(mean)	0.359(2)
Phase shift	0.035(5)
Hotter star	
Colatitude$_{\rm spot}$(deg)	104(2)
Longitude$_{\rm spot}$(deg)	127(2)
Radius$_{\rm spot}$(deg)	32(1)
$T_{\rm spot}/T_{\rm star}$	1.13(1)
Cooler star	
Colatitude$_{\rm spot}$(deg)	59(3)
Longitude$_{\rm spot}$(deg)	69(2)
Radius$_{\rm spot}$(deg)	38(1)
$T_{\rm spot}/T_{\rm star}$	1.17(1)

improved with the optimizing section of the code. We evaluated all binary types to do the light curve analysis and found that only the "semi-detached binary with primary star fills Roche lobe" model produces the best and most logical results. $g_h = g_c = 0.32$ (Lucy 1967) and $A_h = A_c = 0.5$ (Ruciński 1969) were used as the bolometric albedo and gravity-darkening coefficients. The stellar atmosphere was described using the Castelli & Kurucz (2004) approach, and the limb-darkening coefficients were employed as free parameters in the solutions.

Based on our light curves in the B and V bands and after the necessary calibrations (Høg et al. 2000), we determined the $(B-V)$ of the system to be 0.435 ± 0.005. As a result, the system's effective temperature (T_1) was considered to be 6564 ± 24 K (Flower 1996). The catalogs list different values of $(B-V)$, such as 0.410 (APASS9) and 0.412 (The Hipparcos and Tycho catalogs), with a temperature difference of about 100 K between what was found in this study and what was indicated in the catalogs. We did the initial light curve analysis after fixing the temperature derived from our $(B-V)$ for the hotter star. Then, using the optimizing section of PHOEBE, we obtained the temperatures of the stars used in the main photometric light curve solutions.

Using relation 1, the mean fractional radii of the components were computed. Also, we calculated fillout factors from the output parameters of the PHOEBE solutions by relation 2.

$$r_{\rm mean} = (r_{\rm back} \times r_{\rm side} \times r_{\rm pole})^{1/3} \quad (1)$$

$$f = \frac{\Omega(L_1) - \Omega}{\Omega(L_1) - \Omega(L_2)} \quad (2)$$

The results of the light curve solutions of the V Gru system are presented in Table 1. The observed and synthetic light curves with residuals are displayed in Figure 2.

The well-known O'Connell effect (O'Connell 1951) is represented by the asymmetry in the brightness of maxima in the light curve of eclipsing binary systems. The O'Connell effect can be recognized in the light curves from our ground-based observations and TESS data. The light curve solutions in this study need two hot star spots on each of the hotter and cooler components. Figure 3 shows a three-dimensional view of V Gru as well as the Roche lobe configuration.

4. Orbital Period Variations

To determine the new times of minima and uncertainties, we utilized Python code using a Gaussian function and the Markov Chain Monte Carlo (MCMC) approach (Poro et al. 2021). The minimum times in the previous studies and in this study were used to get the potential orbital period change using mid-eclipse times. For this, TIming DAtabase at Krakow (TIDAK) was also taken into account (Tables 2 and A1). In collecting mid-eclipse times in previous reports, we used only those observed with the CCD cameras. All times of minima are expressed in Barycentric Julian Date in Barycentric Dynamical Time ($\rm BJD_{TDB}$).

In this study, a total of seven minima, four primary (Min.I) and three secondary (Min.II), were obtained separately for V Gru from BVI ground-based observations (Table 2). Since we recorded no color dependence on the timings, we averaged the data acquired from all filters. The reference ephemeris (Richards et al. 2021) is used for calculating epoch and O-C

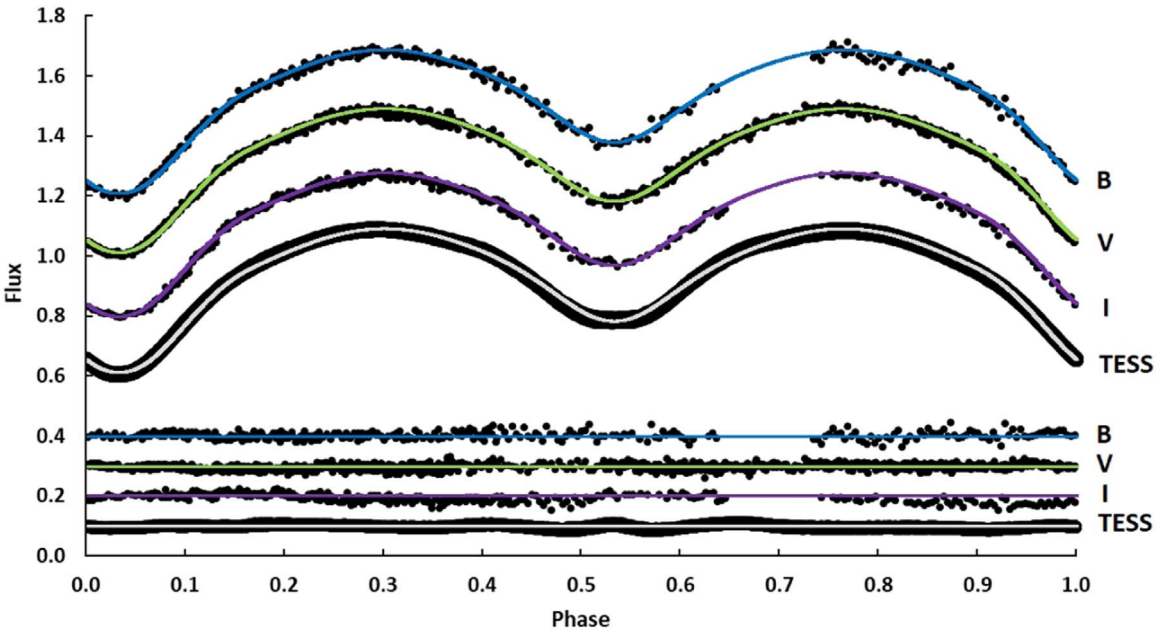

Figure 2. V Gru observational light curves (points) and modeled solutions (lines) are presented with respect to the orbital phase and shifted arbitrarily in the relative flux.

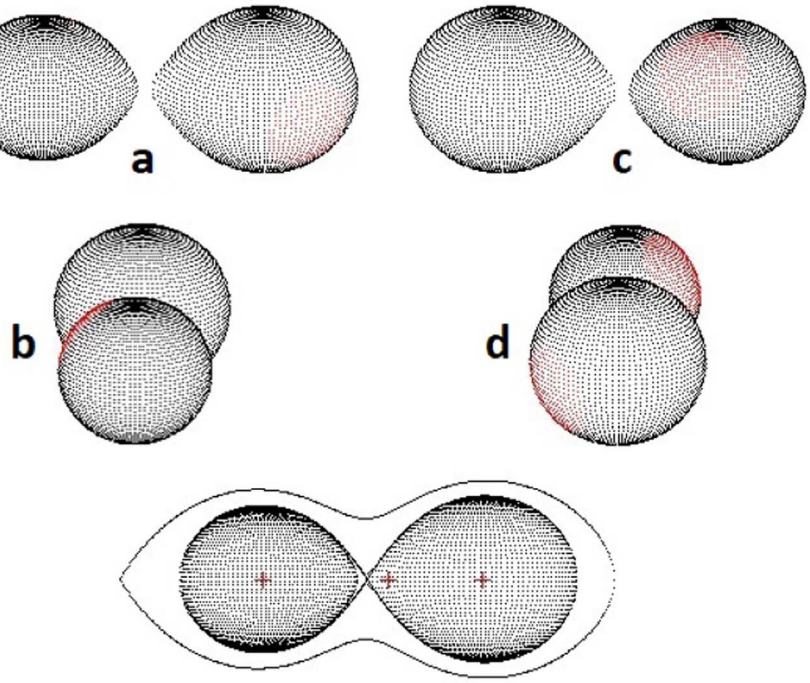

Figure 3. The positions of the components of the V Gru system and the cross-sectional outline of the binary system.

of mid-eclipse times

$$\mathrm{BJD_{TDB}(Min.}I) = 2458727.99696(10) + 0.4834461(5) \times E. \quad (3)$$

This study provided a total of 196 mid-eclipse timings for V Gru, including 184 extracted from TESS data, listed in Tables 2 and the appendix table. We used the MCMC approach to obtain a new ephemeris for the system (e.g., Poro et al. 2022). We find

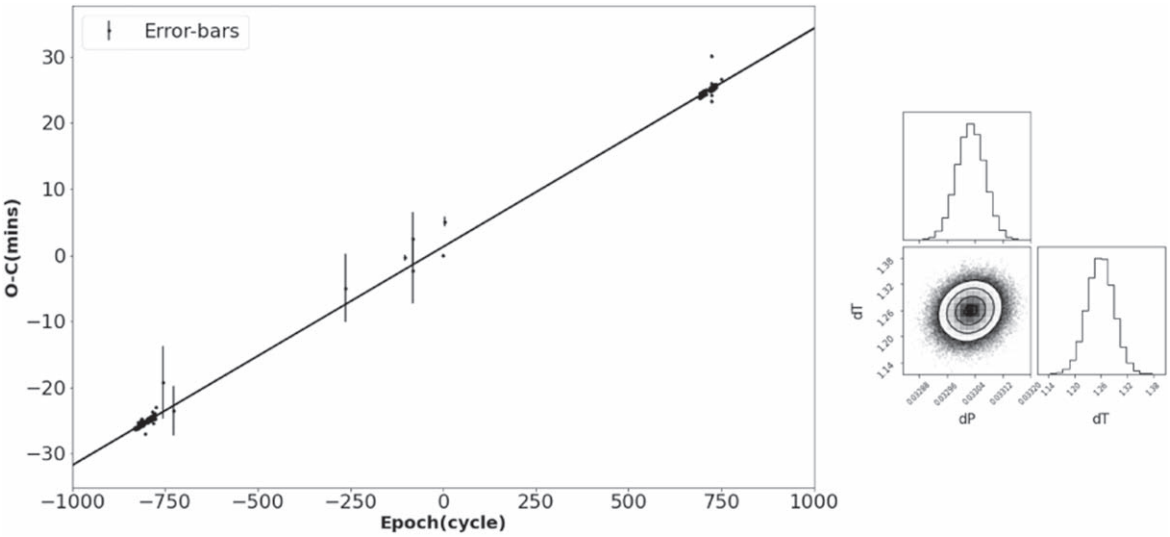

Figure 4. (Left) The *O–C* diagram of the V Gru system with a linear fit to the data points. (Right) Corner plots of the posterior distribution based on the MCMC sampling.

Table 2
Mid-eclipse Times Based on *BVI* Observations of this Study

Min.(BJD_{TDB})	Error	Filter	Epoch	*O–C*
2459078.02872	0.00016	*V*	724	0.0168
2459078.02965	0.00016	*B*	724	0.0177
2459078.02997	0.00017	*I*	724	0.0180
2459090.11660	0.00004	*V*	749	0.0185
2459078.26981	0.00021	*I*	724.5	0.0162
2459078.27130	0.00030	*V*	724.5	0.0176
2459078.27458	0.00021	*B*	724.5	0.0209

the revised period to be 0.483469038 days for the V Gru system. Figure 4 shows the $O-C$ diagram of the system. A new revised linear ephemeris for the mid-eclipse timings obtained from this study, TESS, and collected from the literature was generated with the following light elements

$$\mathrm{BJD_{TDB}(Min.}I) = 2458727.99791^{+(5)}_{-(4)} + 0.483469038^{+(52)}_{-(50)} \times E. \quad (4)$$

5. Conclusion

The V Gru short-period binary system was photometrically observed during a period of 15 nights at a southern hemisphere observatory using *BVI* filters. We extracted minima times from our observations and TESS data, together with additional minima times from the literature; a new ephemeris for the system was presented using the MCMC approach. The $O-C$ diagram shows an increasing and linear trend.

To analyze the light curves of this system, PHOEBE codes were employed. The two components have a 1239 K temperature differential, according to Allen's table (Cox 2000); these temperatures suggest that the spectral types of the hotter and cooler components are F2 and G8, respectively.

The appearance of the light curve is typically the basis for classifications related to machine learning, such as the machine-learned ASAS classification catalog (Richards et al. 2012). Classifications are generally designed with the aim of examining systems for which detailed analysis has not yet been provided and appropriate information is not yet available. As a result, they cannot be trusted in systems like V Gru. This may be one of the classifier's faults, which is a problem that artificial intelligence (AI) is hoping to solve in the future. It appears that a different classification offered by Kopal (1955) based on the relationship of the components to their surrounding Roche lobes is currently preferred.

The short orbital period and light curve analysis of V Gru shows that this binary system is a near-contact eclipsing binary with a negative fillout factor for the cooler component. So, the hotter component has filled its Roche lobe, but the cooler star has not yet filled it. However, this system needs investigation with further observations, including spectroscopic analysis.

Acknowledgments

This manuscript was prepared based on a cooperation between the Binary Systems of the South and North (BSN) Project, the astronomy department of the Raderon AI Lab., and Erciyes University Scientific Research Projects Coordination Unit (Project No. 11737). In this work, we used Gaia DR3 data

from the European Space Agency (ESA) mission Gaia (http://www.cosmos.esa.int/gaia). The SIMBAD database, operated by CDS, Strasbourg, France, has been used in this study. The National Science Foundation (NSF 1 517 474, 1 909 109) and the National Aeronautics and Space Administration (NASA 17-ADAP17-68) both contributed funding to PHOEBE that we utilized. We are especially grateful to Prof. Edwin Budding for his valuable comments.

Data Availability

The data used in this study are available in the online version of this paper.

Appendix A

Mid-eclipse times extracted from TESS observations as well as compiled from the literature are given in Table A1.

Table A1
Available Mid-eclipse Times of V Gru Obtained by CCD

Min.(BJD_{TDB})	Error	Epoch	*O–C*	Ref.	Min.(BJD_{TDB})	Error	Epoch	*O–C*	Ref.
2458325.50990	0.00002	−832.5	−0.0182	TESS	2458335.17979	0.00003	−812.5	−0.0172	TESS
2458325.75160	0.00001	−832	−0.0182	TESS	2458335.42087	0.00001	−812	−0.0179	TESS
2458325.99345	0.00003	−831.5	−0.0181	TESS	2458335.66310	0.00003	−811.5	−0.0173	TESS
2458326.23501	0.00001	−831	−0.0182	TESS	2458335.90437	0.00001	−811	−0.0178	TESS
2458326.47681	0.00003	−830.5	−0.0182	TESS	2458336.14657	0.00002	−810.5	−0.0173	TESS
2458326.71852	0.00001	−830	−0.0182	TESS	2458336.38772	0.00001	−810	−0.0179	TESS
2458326.96029	0.00002	−829.5	−0.0181	TESS	2458336.62999	0.00003	−809.5	−0.0174	TESS
2458327.20183	0.00002	−829	−0.0183	TESS	2458336.87126	0.00001	−809	−0.0178	TESS
2458327.44362	0.00003	−828.5	−0.0182	TESS	2458337.11338	0.00003	−808.5	−0.0174	TESS
2458327.68548	0.00001	−828	−0.0181	TESS	2458337.35473	0.00001	−808	−0.0178	TESS
2458327.92716	0.00003	−827.5	−0.0182	TESS	2458337.59681	0.00002	−807.5	−0.0174	TESS
2458328.16892	0.00001	−827	−0.0181	TESS	2458337.83819	0.00002	−807	−0.0178	TESS
2458328.41065	0.00002	−826.5	−0.0181	TESS	2458338.08006	0.00002	−806.5	−0.0176	TESS
2458328.65233	0.00001	−826	−0.0182	TESS	2458338.32176	0.00001	−806	−0.0176	TESS
2458328.89421	0.00003	−825.5	−0.0180	TESS	2458339.77100	0.00001	−803	−0.0187	TESS
2458329.13572	0.00001	−825	−0.0182	TESS	2458340.01388	0.00002	−802.5	−0.0176	TESS
2458329.37761	0.00002	−824.5	−0.0180	TESS	2458340.25563	0.00001	−802	−0.0176	TESS
2458329.61914	0.00001	−824	−0.0182	TESS	2458340.49740	0.00002	−801.5	−0.0175	TESS
2458329.86095	0.00003	−823.5	−0.0181	TESS	2458340.73909	0.00001	−801	−0.0175	TESS
2458330.10266	0.00002	−823	−0.0182	TESS	2458340.98100	0.00003	−800.5	−0.0174	TESS
2458330.34502	0.00003	−822.5	−0.0175	TESS	2458341.22263	0.00001	−800	−0.0174	TESS
2458330.58617	0.00001	−822	−0.0181	TESS	2458341.46439	0.00003	−799.5	−0.0174	TESS
2458330.82825	0.00003	−821.5	−0.0177	TESS	2458341.70599	0.00002	−799	−0.0175	TESS
2458331.06959	0.00001	−821	−0.0181	TESS	2458341.94791	0.00002	−798.5	−0.0173	TESS
2458331.31153	0.00002	−820.5	−0.0179	TESS	2458342.18946	0.00001	−798	−0.0175	TESS
2458331.55305	0.00001	−820	−0.0181	TESS	2458342.43148	0.00003	−797.5	−0.0172	TESS
2458331.79493	0.00002	−819.5	−0.0180	TESS	2458342.67290	0.00001	−797	−0.0175	TESS
2458332.03660	0.00002	−819	−0.0180	TESS	2458342.91491	0.00002	−796.5	−0.0172	TESS
2458332.27842	0.00002	−818.5	−0.0179	TESS	2458343.15636	0.00001	−796	−0.0175	TESS
2458332.52004	0.00001	−818	−0.0180	TESS	2458343.39840	0.00003	−795.5	−0.0172	TESS
2458332.76213	0.00003	−817.5	−0.0176	TESS	2458343.63983	0.00001	−795	−0.0175	TESS
2458333.00348	0.00001	−817	−0.0180	TESS	2458343.88194	0.00003	−794.5	−0.0171	TESS
2458333.24561	0.00002	−816.5	−0.0176	TESS	2458344.12327	0.00001	−794	−0.0175	TESS
2458333.48702	0.00001	−816	−0.0179	TESS	2458344.36540	0.00003	−793.5	−0.0171	TESS
2458333.72912	0.00003	−815.5	−0.0175	TESS	2458344.60673	0.00001	−793	−0.0175	TESS
2458333.97043	0.00001	−815	−0.0180	TESS	2458344.84880	0.00003	−792.5	−0.0171	TESS
2458334.21272	0.00003	−814.5	−0.0174	TESS	2458345.09025	0.00001	−792	−0.0174	TESS
2458334.45392	0.00001	−814	−0.0179	TESS	2458345.33227	0.00003	−791.5	−0.0171	TESS
2458334.69611	0.00002	−813.5	−0.0174	TESS	2458345.57372	0.00001	−791	−0.0174	TESS
2458334.93736	0.00001	−813	−0.0179	TESS	2458345.81567	0.00002	−790.5	−0.0171	TESS
2458346.05722	0.00001	−790	−0.0173	TESS	2459063.52512	0.00001	694	0.0166	TESS
2458346.29922	0.00003	−789.5	−0.0170	TESS	2459063.76726	0.00002	694.5	0.0170	TESS
2458346.54072	0.00001	−789	−0.0173	TESS	2459064.00865	0.00001	695	0.0167	TESS
2458346.78271	0.00003	−788.5	−0.0170	TESS	2459064.25078	0.00002	695.5	0.0171	TESS
2458347.02407	0.00001	−788	−0.0174	TESS	2459064.49211	0.00001	696	0.0167	TESS
2458347.26602	0.00003	−787.5	−0.0171	TESS	2459064.73422	0.00002	696.5	0.0171	TESS
2458347.50800	0.00001	−787	−0.0169	TESS	2459064.97558	0.00001	697	0.0167	TESS
2458347.99100	0.00001	−786	−0.0173	TESS	2459065.21769	0.00002	697.5	0.0171	TESS

Table A1
(Continued)

Min.(BJD_{TDB})	Error	Epoch	*O*–*C*	Ref.	Min.(BJD_{TDB})	Error	Epoch	*O*–*C*	Ref.
2458348.47536	0.00005	−785	−0.0164	TESS	2459065.45906	0.00001	698	0.0167	TESS
2458348.95822	0.00005	−784	−0.0170	TESS	2459065.70110	0.00002	698.5	0.0170	TESS
2458349.44100	0.00001	−783	−0.0177	TESS	2459065.94251	0.00001	699	0.0167	TESS
2458349.68364	0.00003	−782.5	−0.0167	TESS	2459066.18458	0.00002	699.5	0.0171	TESS
2458349.92493	0.00001	−782	−0.0172	TESS	2459066.42605	0.00001	700	0.0168	TESS
2458350.16688	0.00003	−781.5	−0.0170	TESS	2459066.66808	0.00002	700.5	0.0171	TESS
2458350.40842	0.00001	−781	−0.0171	TESS	2459066.90959	0.00001	701	0.0169	TESS
2458350.65038	0.00003	−780.5	−0.0169	TESS	2459067.15163	0.00002	701.5	0.0172	TESS
2458350.89183	0.00001	−780	−0.0172	TESS	2459067.39294	0.00001	702	0.0168	TESS
2458351.13379	0.00002	−779.5	−0.0169	TESS	2459067.63503	0.00002	702.5	0.0172	TESS
2458351.37526	0.00001	−779	−0.0172	TESS	2459067.87636	0.00001	703	0.0168	TESS
2458351.61747	0.00003	−778.5	−0.0167	TESS	2459068.11850	0.00002	703.5	0.0172	TESS
2458351.85874	0.00001	−778	−0.0172	TESS	2459068.35982	0.00001	704	0.0168	TESS
2458352.10074	0.00003	−777.5	−0.0169	TESS	2459068.60201	0.00002	704.5	0.0173	TESS
2458352.34218	0.00001	−777	−0.0172	TESS	2459068.84332	0.00001	705	0.0169	TESS
2458352.58441	0.00003	−776.5	−0.0167	TESS	2459069.08546	0.00002	705.5	0.0173	TESS
2458352.82562	0.00001	−776	−0.0172	TESS	2459069.32683	0.00001	706	0.0169	TESS
2458353.06853	0.00003	−775.5	−0.0160	TESS	2459069.56887	0.00002	706.5	0.0172	TESS
2458362.98178	0.00380	−755	−0.0134	Richards et al. (2021)	2459069.81025	0.00001	707	0.0169	TESS
2458376.99878	0.00260	−726	−0.0163	Richards et al. (2021)	2459070.05236	0.00002	707.5	0.0173	TESS
2458600.84718	0.00360	−263	−0.0035	TIDAK	2459070.29378	0.00001	708	0.0170	TESS
2458678.20175	0.00031	−103	−0.0003	Richards et al. (2021)	2459070.53592	0.00002	708.5	0.0174	TESS
2458688.11438	0.00280	−82.5	0.0017	TIDAK	2459070.77718	0.00001	709	0.0169	TESS
2458688.35277	0.00350	−82	−0.0016	TIDAK	2459071.01930	0.00002	709.5	0.0173	TESS
2458727.99696	0.00010	0	0	Richards et al. (2021)	2459075.37048	0.00002	718.5	0.0175	TESS
2458730.17597	0.00052	4.5	0.0035	Richards et al. (2020)	2459075.61194	0.00001	719	0.0172	TESS
2459062.07470	0.00001	691	0.0165	TESS	2459075.85395	0.00002	719.5	0.0175	TESS
2459062.31694	0.00002	691.5	0.0170	TESS	2459076.09541	0.00001	720	0.0173	TESS
2459062.55821	0.00001	692	0.0165	TESS	2459076.33734	0.00002	720.5	0.0175	TESS
2459062.80034	0.00002	692.5	0.0170	TESS	2459076.57882	0.00001	721	0.0172	TESS
2459063.04162	0.00001	693	0.0165	TESS	2459076.82085	0.00002	721.5	0.0175	TESS
2459063.28382	0.00002	693.5	0.0170	TESS	2459077.06236	0.00001	722	0.0173	TESS
2459077.30438	0.00002	722.5	0.0176	TESS	2459080.93009	0.00001	730	0.0175	TESS
2459077.54585	0.00001	723	0.0174	TESS	2459081.17185	0.00002	730.5	0.0175	TESS
2459077.78791	0.00002	723.5	0.0177	TESS	2459081.41355	0.00001	731	0.0175	TESS
2459078.02924	0.00001	724	0.0173	TESS	2459081.65566	0.00002	731.5	0.0179	TESS
2459078.27126	0.00002	724.5	0.0176	TESS	2459081.89704	0.00001	732	0.0175	TESS
2459078.51272	0.00001	725	0.0173	TESS	2459082.13905	0.00002	732.5	0.0178	TESS
2459078.75480	0.00002	725.5	0.0177	TESS	2459082.38055	0.00001	733	0.0176	TESS
2459078.99621	0.00001	726	0.0174	TESS	2459082.62257	0.00002	733.5	0.0179	TESS
2459079.23824	0.00002	726.5	0.0177	TESS	2459082.86399	0.00001	734	0.0176	TESS
2459079.47966	0.00001	727	0.0174	TESS	2459083.10602	0.00002	734.5	0.0179	TESS
2459079.72164	0.00002	727.5	0.0176	TESS	2459083.34745	0.00001	735	0.0176	TESS
2459079.96311	0.00001	728	0.0174	TESS	2459083.58949	0.00002	735.5	0.0179	TESS
2459080.20524	0.00002	728.5	0.0178	TESS	2459083.83091	0.00001	736	0.0176	TESS
2459080.44660	0.00001	729	0.0174	TESS	2459084.07287	0.00002	736.5	0.0179	TESS
2459080.68867	0.00002	729.5	0.0178	TESS					

ORCID iDs

Mehmet Tanriver https://orcid.org/0000-0002-3263-9680
Atila Poro https://orcid.org/0000-0002-0196-9732
Ahmet Bulut https://orcid.org/0000-0002-7215-926X
Ahmet Keskin https://orcid.org/0000-0002-9314-0648
Mark G. Blackford https://orcid.org/0000-0003-0524-2204

References

Avvakumova, E. A., Malkov, O. Y., & Kniazev, A. Y. 2013, AN, 334, 860
Budding, E. 1984, BICDS, 27, 91
Budding, E., Erdem, A., Çiçek, C., et al. 2004, A&A, 417, 263
Cannon, A. J., & Pickering, E. C. 1993, yCat, III/135A
Castelli, F., & Kurucz, R. L. 2004, A&A, 419, 725
Collins, K. A., Kielkopf, J. F., Stassun, K. G., & Hessman, F. V. 2017, AJ, 153, 77
Conroy, K. E., Kochoska, A., Hey, D., et al. 2020, ApJS, 250, 34
Cox, A. N. 2000, Allen's Astrophysical Quantities (NASA: NASA Astrophysics Data System)
Cruzalèbes, P., Petrov, R. G., Robbe-Dubois, S., et al. 2019, MNRAS, 490, 3158
Demartino, R., Kocyla, D., Predom, C., & Wetherbee, E. 1996, IBVS, 4321, 1
Flower, P. J. 1996, ApJ, 469, 355
George, D. B. 2000, IAPPP, 79, 2
Giuricin, G., Mardirossian, F., & Mezzetti, M. 1983, A&As, 54, 211
Hauck, B., & Mermilliod, M. 1998, A&As, 129, 431
Høg, E., Fabricius, C., Makarov, V. V., et al. 2000, A&A, 357, 367
Houk, N. 1978, Michigan Catalog of Two-Dimensional Spectral Types for the HD Stars, Vol. 2, University of Michigan
Jenkins, J. M., Twicken, J. D., McCauliff, S., et al. 2016, Proc. SPIE, 9913, 99133E
Kopal, Z. 1955, AnAp, 18, 379
Kordopatis, G., Gilmore, G., Steinmetz, M., et al. 2013, AJ, 146, 134
Kunder, A., Kordopatis, G., Steinmetz, M., et al. 2017, AJ, 153, 75
Leavitt, H. S., & Pickering, E. C. 1913, HarCi, 179, 1
Lopez, C. E., & Lepez, H. S. 2000, IBVS, 4824, 1
Lucy, L. B. 1967, ZAp, 65, 89
Mason, B. D., Wycoff, G. L., Hartkopf, W. I., Douglass, G. G., & Worley, C. E. 2001, AJ, 122, 3466
O'Connell, D. J. K. 1951, PRCO, 2, 85
Paunzen, E. 2015, A&A, 580, A23
Poro, A., Paki, E., Blackford, M. G., et al. 2022, PASP, 134, 064201
Poro, A., Zamanpour, S., Hashemi, M., et al. 2021, NewA, 86, 101571
Prša, A., & Zwitter, T. 2005, ApJ, 628, 426
Richards, J. W., Starr, D. L., Miller, A. A., et al. 2012, ApJS, 203, 32
Richards, T., Axelsen, R. A., Blackford, M., Jenkins, R., & Moriarty, D. J. W. 2021, JAAVSO, 49, 251
Richards, T., Blackford, M., Butterworth, N., & Jenkins, R. 2020, JAAVSO, 48, 250
Ruciński, S. M. 1969, AcA, 19, 245
Steinmetz, M., Guiglion, G., McMillan, P. J., et al. 2020, AJ, 160, 83
Wolf, G. W., & Kern, J. T. 1983, ApJS, 52, 429
Wolf, G. W., Kern, J. T., Hayes, T. L., & Chaffin, C. R. 1982, IBVS, 2185, 1